# Nanoscopic Surface Patterns from Functional ABC Triblock Copolymers

**Alexander Böker,[†,‡] Axel H. E. Müller,[†,§] and Georg Krausch*[,‡,§]**

*Lehrstuhl für Makromolekulare Chemie II, Lehrstuhl für Physikalische Chemie II, and Bayreuther Zentrum für Kolloide und Grenzflächen, Universität Bayreuth, D-95440 Bayreuth, Germany*

*Received December 27, 2000*

ABSTRACT: We synthesized analogous series of monodisperse ABC triblock copolymers with symmetrical end blocks A/C and different short middle blocks B (5−10 wt %) with varying polarities by sequential anionic polymerization, i.e., polystyrene-*b*-poly(2-vinylpyridine)-*b*-poly(methyl methacrylate) (PS-*b*-P2VP-*b*-PMMA) and polystyrene-*b*-poly(2-hydroxyethyl methacrylate)-*b*-poly(methyl methacrylate) (PS-*b*-PHEMA-*b*-PMMA). Thin (thickness ∼ 20 nm) and ultrathin films (thickness ≤ 7 nm) were prepared by either dip-coating or adsorption from solution onto silicon wafers. The copolymer films were investigated by scanning force microscopy. In thin films, the polar middle block adsorbs preferentially to the polar substrate, resulting in a polymer film surface that exclusively consists of PS and PMMA microdomains. In ultrathin films, the two polar B and C blocks behave like a single B block resulting in structures which can be described by recent scaling laws. The lateral spacing and the morphology of the structures can be controlled by film thickness and A/C block length.

## Introduction

In recent years, the use of block copolymers for surface patterning has attracted increasing attention.[1−5] Well-defined laterally patterned surfaces are important for a variety of technological applications, e.g., as compatibilizers for polymer blends or as templates for growing biological cells with controlled shapes and sizes.[6] In addition, patterned polymer substrates can also be used as templates in fabrication of optoelectronic devices through the selective adsorption of a conducting material,[7] which results in a system of alternating polymeric and metallic stripes with domain spacings in the tens of nanometers scale, an order of magnitude smaller than typically achieved through photolithography. The high potential of polymer-patterned substrates for lithographic purposes has recently been demonstrated by Spatz et al., who deposited polystyrene-*b*-poly(2-vinylpyridine) (PS-*b*-P2VP) block copolymers on mica and created highly ordered hexagonal arrays of PS dots on the surface. These were used as templates for lithographic masks.[8,9] Aside from these practical applications, laterally patterned polymer surfaces can be of use as model systems for the study of wetting and dewetting phenomena on heterogeneous substrates.[10]

To this point, most of the experiments described in the literature involved diblock copolymers only, disregarding the potential advantage of ABC triblock copolymers for the generation of lateral structures in thin films. The latter was recently pointed out by Pickett and Balazs in the context of self-consistent-field calculations for the case of symmetric ABC triblock copolymers.[11] The authors showed that a perpendicular alignment of the lamellae with respect to the plane of the films is expected, when the boundary surfaces preferentially attract the middle block B. In the case of a sufficiently strong interaction between the walls and the adsorbing block B, the A and C end blocks may even be expelled from the walls, resulting in homogeneous layers of B next to the walls and a laterally microphase-separated layer of A and C in the film center. Given that the end blocks have a lower surface energy than the middle block B, these results suggest that one may remove one of the walls and expect that the film structure consists of a homogeneous B layer adsorbed at the substrate covered with a laterally microphase-separated A/C striped surface layer. First experiments along these lines were recently reported.[12]

The aim of the present work is to generate striped surfaces of controlled size and domain spacing in the nanometer range by use of suitably chosen ABC triblock copolymers. Control over the lateral dimensions is gained by variation of film thickness and A/C block length. Thin and ultrathin films of two series of block copolymers are investigated by tapping mode SFM. The experimental results are discussed in view of recent scaling considerations developed in the context of pattern formation in diblock copolymer thin films.[13,14]

## Experimental Section

The block copolymers were synthesized by sequential anionic polymerization (Scheme 1). The deprotection of the hydroxyl group of the PHEMA block was accomplished by precipitating the polymer into technical grade methanol. Gel permeation chromatography (GPC) proved that the polymerization yielded monodisperse triblock copolymers (Figure 1). The functional block copolymers were synthesized to give two series of polymers with constant relative amounts of polystyrene, poly(methyl methacrylate) (∼45 wt %) and the functional middle block (consisting of 5−10 wt % poly(2-hydroxyethyl methacrylate) or poly(2-vinylpyridine), respectively). In each series only the overall molecular weight of the whole block copolymer was varied as shown in Table 1. The composition was calculated from $^1$H NMR of the block copolymer using GPC results for the corresponding PS precursor, calibrated with narrowly distributed PS standards.

**Solvents and Materials.** Unless noted, all chemicals were purchased from Aldrich and used without further purification.

Styrene was stirred twice over calcium hydride for 24 h, and finally, after overnight treatment with $MgBu_2$ (bright yellowish color), it has been condensed into an ampule and set under nitrogen for storage.

* Corresponding author. E-mail: georg.krausch@uni-bayreuth.de.
† Lehrstuhl für Makromolekulare Chemie II, Universität Bayreuth.
‡ Lehrstuhl für Physikalische Chemie II, Universität Bayreuth.
§ Bayreuther Zentrum für Kolloide und Grenzflächen, Universität Bayreuth.

10.1021/ma002198d CCC: $20.00 
Published on Web 09/12/2001

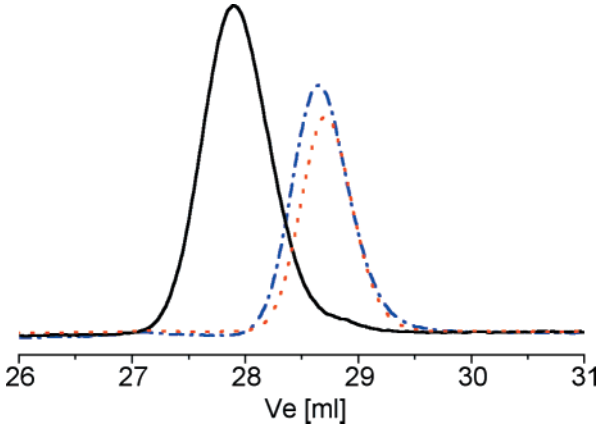


**Figure 1.** GPC trace (RI signal) of triblock copolymer $S_{47}H_{10}M_{43}^{82}$ (—) and its precursors PS (•••) and PS-*b*-PHEMA (• - •). $M_n$ = 82 300 g/mol; $M_w/M_n$ = 1.04.

**Scheme 1. Synthesis of PS-*b*-PHEMA-*b*-PMMA (SHM) Triblock Copolymers**

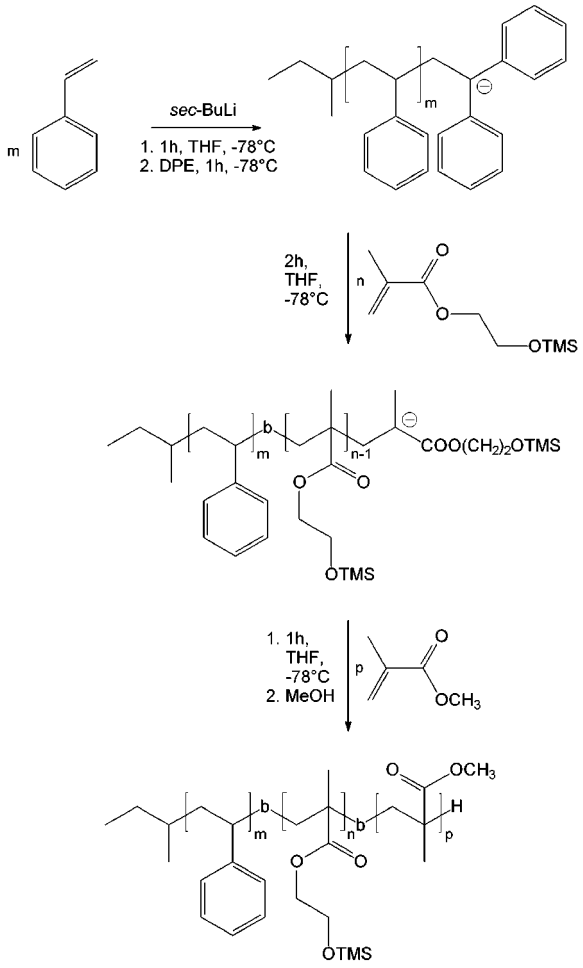


Trimethylsilyl-protected 2-hydroxyethyl methacrylate (TMS−HEMA) was stirred twice over calcium hydride for 24 h and purified by reduced pressure distillation. Prior to use, it was filtered over a 1 cm column filled with neutral alumina.

2-Vinylpyridine was treated with triethyl aluminum for 3 h and condensed into a Schlenk flask, from which it was taken directly for the polymerization procedure.

Methyl methacrylate was stirred with triethyl aluminum for 2 h, condensed into a glass ampule and finally stored under nitrogen.

The solvent tetrahydrofuran (THF) was distilled over calcium hydride for 48 h and finally refluxed over potassium under nitrogen for another 2 days.

**Table 1. GPC Data for the Synthesized Block Copolymers[a]**

| polymer | $M_n$(S) [kg/mol] | $M_n$(H/2VP) [kg/mol] | $M_n$(M) [kg/mol] | $M_w/M_n$ (GPC) | $\Sigma M_n$(total) [kg/mol] |
|---|---|---|---|---|---|
| $S_{47}H_{10}M_{43}^{82}$ | 38.7 | 8.4 | 35.2 | 1.04 | 82.3 |
| $S_{46}H_4M_{50}^{134}$ | 61.5 | 5.2 | 67.7 | 1.06 | 134.4 |
| $S_{67}H_6M_{27}^{129}$ | 86.4 | 8.0 | 34.1 | 1.02 | 128.5 |
| $S_{51}2VP_5M_{44}^{110}$ | 56.2 | 5.9 | 48.2 | 1.06 | 110.3 |
| $S_{48}2VP_5M_{47}^{180}$ | 85.8 | 8.6 | 85.5 | 1.05 | 179.9 |
| $S_{56}2VP_6M_{38}^{299}$ | 168.4 | 16.6 | 113.6 | 1.05 | 298.6 |

[a] The subscript indicates the weight fraction of the corresponding blocks. The superscript denotes the total $M_n$ in kg/mol.

**Synthesis of 2-[(Trimethylsilyl)oxy]ethyl methacrylate (TMS−HEMA).** The trimethylsilyl protecting group was introduced as previously reported by Hirao et al.[15] using hexamethyldisilazane and trimethylsilyl chloride.

**Block Copolymerizations.** A 1 L aliquot of freshly distilled THF was cooled to −78 °C. Then, 0.36 mL of *sec*-BuLi (1.55 molar solution in *n*-hexane/cyclohexane) was injected, before 23.4 g of styrene was added. After 60 min of polymerization, the styryl anions were capped with 0.17 mL of 1,1-diphenylethylene (DPE), which results in a deep red color of the reaction mixture. One hour later, the polymerization was resumed by injection of 7.9 mL (7.3 g) of TMS−HEMA, which leads to immediate disappearance of the red color. After additional 2 h, 24 g of MMA were added quickly and polymerized for another 45 min. Finally, the reaction was terminated with 1 mL of degassed methanol.

The polymer was precipitated in 5 L of methanol, which also leads to deprotection of the PHEMA block. Then the product was redissolved in THF and reprecipitated two more times into 2-propanol and dried under vacuum at room temperature.

A similar procedure was chosen for the preparation of the polystyrene-*b*-poly(2-vinylpyridine)-*b*-poly(methyl methacrylate) block copolymers. After capping the styryl anions with DPE, the 2-vinylpyridine was allowed to polymerize for 1 h. Before addition of MMA, DPE was added again and reacted overnight in order to achieve a complete capping reaction.

The block ratio was determined by $^1$H NMR spectra using the integrated aromatic signals of the polystyrene block in combination with the GPC results of the styrene precursor.

**Polymer Analysis.** GPC measurements were performed using a set of 30 cm SDV-gel columns of 5 $\mu$m particle size having $10^5$, $10^4$, $10^3$, and $10^2$ Å pore size and dual detectors (RI and UV [$\lambda$ = 254 nm]). The solvent was THF at room temperature with an elution rate of 1 mL/min. Narrowly distributed polystyrene samples were used as calibration standards.

$^1$H NMR spectra were acquired on a 250 MHz Bruker AC 250 instrument using $CDCl_3$ or THF-$d_8$ as solvents and tetramethylsilane (TMS) as internal standard. The molecular weights of the B and C blocks were calculated using the block copolymer composition determined by NMR and the polystyrene molecular weights obtained from GPC.

**Sample Preparation.** Thin polymer films were prepared on polished silicon wafers by dip-coating from 1 mg/mL solutions of the block copolymers in THF. To study ultrathin films, the silicon wafers were exposed to 1 mg/mL solutions of the polymers for 3−4 days, which led to adsorption of the block copolymer onto the polar substrate. Subsequently, the wafers were rinsed four times with 5 mL THF.

Prior to use, the Si wafers were rinsed in organic solvents (THF, chloroform and acetone) and subsequently treated with a beam of $CO_2$ crystals ("snow jet") to remove any organic residues from the surface.

**Scanning Force Microscopy.** SFM images were taken on a Digital Instruments Dimension 3100 microscope operated in tapping mode (free amplitude of the cantilever ≈ 20 nm, amplitude set point ≈ 0.98). The standard silicon nitride probes were driven at 3% offset below their resonance frequencies in the range of 250−350 kHz. Height and phase images were taken at scanning speeds of around 6 $\mu$m/s.

**Scheme 2. Schematic Representation of a Cross Section through an Ultrathin Film of PS-*b*-PMMA Diblock Copolymers Adsorbed onto a Silicon Substrate**

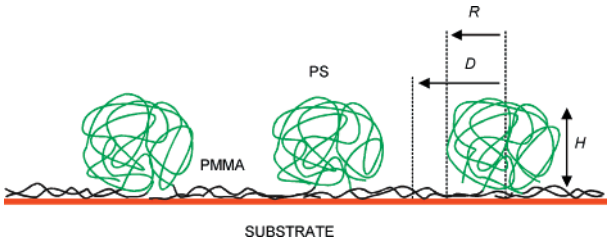


**Transmission Electron Microscopy.** The bulk morphology of the block copolymers was examined using TEM. Films (around 1 mm thick) were cast from 5 wt % solutions in THF and allowed to evaporate slowly for 5 days. The as-cast films were dried for 1 day in a vacuum oven at room temperature followed by annealing at 140 °C for at least 1 week under vacuum. Thin sections were cut at room temperature using a Reichert-Jung Ultracut E microtome equipped with a diamond knife. To enhance the electron density contrast between polystyrene and the methacrylic blocks, the sections were exposed to $RuO_4$ vapor for 45 min, which leads to a preferential staining of the polystyrene block. Bright field TEM was performed using a Zeiss electron microscope (CEM 902) operated at 80 kV.

**Small Angle X-ray Scattering.** SAXS measurements were performed using a Bruker-AXS Nanostar instrument with a Siemens Kristalloflex 760 X-ray source (Cu $K_\alpha$ radiation: 1.541 Å) operated at 40 mA and 40 kV and a 2D Histar detector.

**Scanning Electron Microscopy.** SEM was performed using a LEO 1530 Gemini instrument equipped with a field emission cathode with a lateral resolution of approximately 2 nm. The acceleration voltage was 1 kV. Prior to the measurements the films were stained with $RuO_4$ vapor for 45 min.

**Evaluation of Characteristic Length Scales and Estimation of Experimental Errors.** The lateral spacing of the thin film structures was determined from the reciprocal of the maximum intensity position of the Fourier transform of a 3 × 3 $\mu m^2$ SFM image. The Fourier transform was calculated using the software supplied with the microscope (version 4.42r4). The uncertainty of the lateral dimensions was estimated from the half-width of the peak in the Fourier transform. The film thickness was determined by SFM scans in a region where the polymer film had been partially removed by a scratch. At least 20 single cross sections were taken at different locations at the step.

The lateral patterns in the ultrathin films were evaluated with respect to the mean stripe-to-stripe or island-to-island half-distance $D$, the mean height $H$, the mean island radius or stripe half-width $R$, and the number of aggregated PS chains $n_{PS}$ in an island or defined section of a stripe (see Scheme 2). The mean half-distance $D$ was determined using Fourier transform as described above for the thin film structures. In the case of the uniform stripe morphology, the average of at least 15 single stripe height values obtained from the SFM height images was taken as the mean stripe height $H$. For the island morphology, the tool *Particle Analysis* of the above-mentioned commercial software was used to determine the mean height $H$ from a 3 × 3 $\mu m^2$ SFM height image. In both cases, the experimental uncertainty was estimated from the statistical scattering of the single island/stripe height values.

The mean radius $R$ of the islands was determined applying *Particle Analysis* of the Nanoscope III software 4.42r4 to a 3 × 3 $\mu m^2$ SFM height image with a constant threshold height of 1 nm. The average of at least 15 single stripe half-widths values was taken as the mean stripe half-width $R$. In both cases, the error $\Delta R$ was estimated from the statistical scattering of the single island/stripe $R$ values. For a correct evaluation of the mean radii or half-widths $R$, one has to take into account the convolution with the curvature of the tip apex, which causes a systematic error by enlarging the lateral dimensions of elevated objects by roughly the tip apex, which itself varies by at least 10% between different tips. In this study, tips were changed regularly to avoid artifacts due to tip contamination. We assume that all tips had a tip radius of $t = 10$ nm by which the imaged objects are enlarged. This value was subtracted from the measured radii and half-width values $R$.

**Scheme 3. Schematic Representation of a Stripe Section with a Base of 2*R* × 2*R***

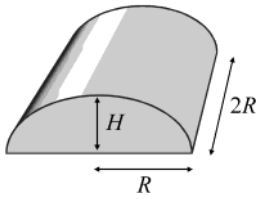


**Table 2. Characteristic Spacings of Phase-Separated Block Copolymers in Bulk and Thin Films as Determined by SFM, TEM, and SAXS**

| polymer | $N_S/N_{H/2VP}/N_M$ | film thickness [nm] | characteristic length scale [nm] SFM | TEM[a] | SAXS[a] |
|---|---|---|---|---|---|
| $S_{47}H_{10}M_{43}^{82}$ | 370/65/350 | 14 ± 2 | 44 ± 4 | 40 ± 4 | 49 ± 6 |
| $S_{46}H_4M_{50}^{134}$ | 590/40/680 | 15 ± 2 | 53 ± 4 | 50 ± 5 | 61 ± 7 |
| $S_{67}H_6M_{27}^{129}$ | 830/60/340 | 12 ± 2 | 58 ± 5 | 49 ± 5[b] | 59 ± 7[b] |
| $S_{51}2VP_5M_{44}^{110}$ | 540/55/480 | 18 ± 2 | 47 ± 5 | 45 ± 5 | 49 ± 6 |
| $S_{48}2VP_5M_{47}^{180}$ | 825/80/855 | 30 ± 4 | 73 ± 8 | 60 ± 6 | 63 ± 8 |
| $S_{56}2VP_6M_{38}^{299}$ | 1620/160/1140 | 25 ± 4 | 92 ± 9 | 80 ± 8 | 80 ± 9 |

[a] Bulk values, all films cast from THF solution. [b] Cylinders.

The number of aggregated PS chains $n_{PS}$ in an island or defined section of a stripe was calculated using the following expressions, assuming a spherical caplike shape of the islands. The volume of a stripe section was modeled as a cylindrical cap with a rectangular base of $2R \times 2R$ and a height $H$ (Scheme 3). For the density of PS we assume $\rho = 1.1$ g/cm$^3$.

(a) Islands:

$$n_{PS,Island} = \frac{\frac{\pi}{6}H(3R^2 + H^2)\rho N_A}{M_n(PS)} \quad (1)$$

(b) Stripes:

$$n_{PS,Stripes} \approx \frac{\left[\frac{(R^2 + H^2)}{H}\left(\sqrt{R^2 + \frac{4}{3}H^2} - R\right) + 2RH\right]R\rho N_A}{M_n(PS)} \quad (2)$$

with $N_A$ and $M_n$(PS) being the Avogadro number and the molecular weight of the PS block, respectively. We note that the estimate for the aggregation number of the stripe pattern $n_{PS,Stripes}$ is based on an approximation for the volume of the cylindrical cap, which leads to an error of less than 3%.

## Results and Discussion

**Bulk Morphology of ABC Block Copolymers.** The bulk morphology of the block copolymers was investigated using TEM and SAXS as described above. All polymers except $S_{67}H_6M_{27}^{129}$ (which shows a cylindrical microdomain structure) exhibit a lamellar morphology with a characteristic lamellar spacing $L_0$ ranging between 40 and 100 nm. The $L_0$ values determined by the two independent methods are shown in Table 2.

**Thin Films of ABC Block Copolymers.** Thin films were produced on polished silicon wafers by dip-coating from dilute (1 mg/mL) solutions of the block copolymers

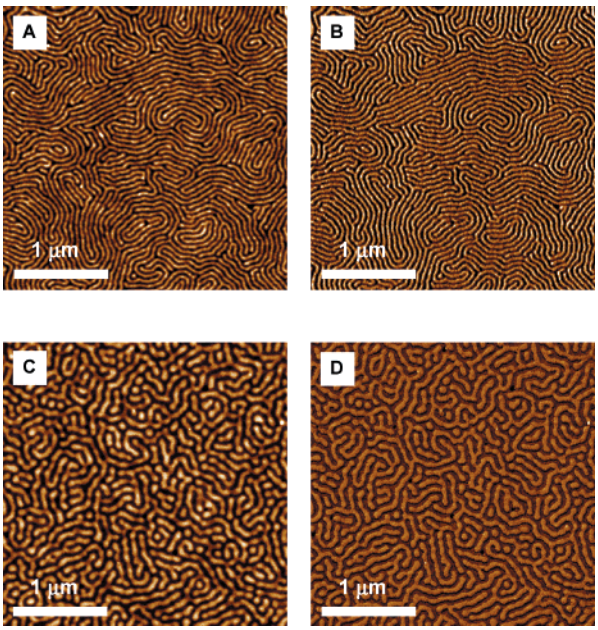


**Figure 2.** SFM topography (a, c) and phase images (b, d) of thin films dip-coated from 1 mg/mL THF solutions onto a polished silicon wafer: (a, b) 15 nm thick film of $S_{46}H_4M_{50}^{134}$; (c, d) 25 nm thick film of $S_{56}2VP_6M_{38}^{299}$. Topography: 8 nm, Phase: 8°.

in tetrahydrofuran (THF). Subsequently, the films were dried at room temperature.

Figure 2a−d shows typical SFM topography and phase images of PS-*b*-PHEMA-*b*-PMMA and PS-*b*-P2VP-*b*-PMMA triblock copolymers. All dip-coated samples exhibit a well-defined wormlike surface structure both in the height and in the phase images. Vacuum annealing (5 d at 140 °C) does not lead to significant changes in surface morphology. The characteristic lateral spacings of all samples were obtained from Fourier transforms of the SFM images as described above. Film thicknesses as determined by SFM scans range between 14 and 30 nm, which is well below $L_0$ for each individual sample (Table 2).

In the following, we shall try to establish a microscopic model of the thin film morphology responsible for the observed surface structures. We expect the polar middle block B (either PHEMA or P2VP) to strongly interact with the native oxide layer on top of the silicon substrate. Therefore, we may assume that only polystyrene (PS) and poly(methyl methacrylate) (PMMA) microdomains are present at the film surface. This notion is supported by the following considerations.

Differences in the solubility of the different components of a block copolymer lead to well-defined topographical features at the film surface.[12,16] It was found that after spin- or dip-coating domains rich in the polymer with the lower solubility tend to protrude over the ones rich in the polymer with the higher solubility. As THF is a slightly better solvent for PS than for PMMA, we expect the PMMA microdomains to protrude over the PS phase. We may therefore identify the protruding features in Figure 2 as PMMA microdomains. The mean height difference between the protrusions (PMMA) and the depressions (PS) ranges between 2 and 4 nm depending on the size of the PS and PMMA blocks of the respective polymer.

This assignment is corroborated by the fact that the protruding domains show a slightly larger phase shift compared to the depressed domains. The average difference in the phase shift between neighboring domains amounts to about 4° (with small variations depending on the tip characteristics and therefore on the measurement conditions). As the harder material commonly exhibits a larger phase shift than a softer material in tapping mode SFM images taken in the repulsive regime, this observation confirms our statement that the protruding phase consists of PMMA.

**Scheme 4. Schematic Depiction of Proposed Surface Perpendicular Morphologies for AB and ABC Block Copolymers**

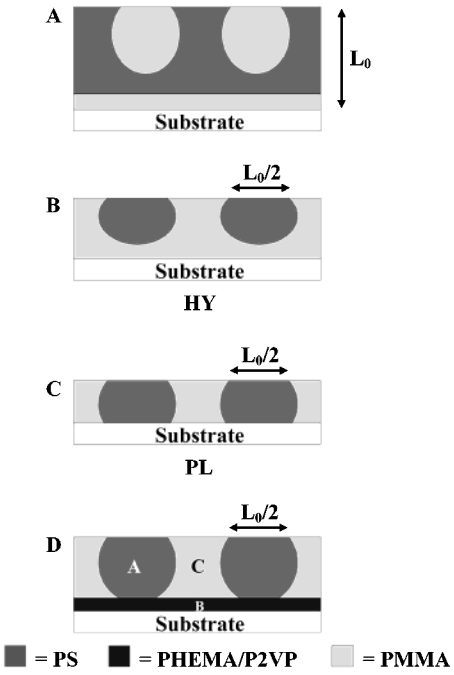


This finding is in agreement with experiments on thin films of PS-*b*-PMMA on silicon nitride.[17] In these experiments, SFM and TEM measurements were performed at the same spot of the sample. The authors showed that, in fact, the PMMA phase protrudes over the PS domains when the samples were prepared from common solvents exhibiting a higher solubility for PS.

Moreover, we observe that the lateral spacings of the thin PS-*b*-PHEMA-*b*-PMMA and PS-*b*-P2VP-*b*-PMMA triblock copolymer films are nearly identical to the ones determined for bulk samples using TEM and SAXS (Table 2). Deviations tend to occur in films of block copolymers with a large amount of PMMA and may be due to degradation of the poly(methacrylates) in the electron beam during the TEM measurements.

Our experiments indicate that the formation of a laterally phase-separated and therefore patterned surface can be accomplished by simple dip-coating from 1 mg/mL THF solutions onto a polished silicon wafer. The patterned regions extend over large areas the size of which mainly depends on the uniformity of film thickness. Aiming toward a model for the microdomain morphology of our samples in the thin film regime, we briefly review related work on diblock copolymers. Morkved et al.[5] observed a kinetically stable perpendicular lamellar structure for symmetric PS-*b*-PMMA diblock copolymers at film thicknesses around one lamellar spacing $L_0$. The authors take into account a possible "capping" of the PS sheets by PMMA at the (polar) substrate (Scheme 4a). Recent self-consistent-field calculations by Fasolka et al.[18] suggest two types of perpendicular morphologies in the thin film regime

for thicknesses below about $^1/_3L_0$, which are depicted in Scheme 4, parts b and c. The authors describe a "hybrid structure" (HY), which consists of a PMMA layer at the substrate/polymer interface with protrusions extending to the polymer/air interface, perforating a PS top layer (Scheme 4b). Alternatively, a so-called "perpendicular lamellae" (PL) morphology is discussed, which consists of full lamellae aligned perpendicular to the plane of the film (Scheme 4c). The calculations predict both (HY and PL) morphologies to exhibit an equilibrium lateral spacing equal to $L_0$.

The latter prediction is also fulfilled by the observations made in the case of the thin PS-*b*-PHEMA-*b*-PMMA and PS-*b*-P2VP-*b*-PMMA triblock copolymer films discussed in the present work. Compared to the situation faced in the above studies, the P2VP/PHEMA middle blocks are expected to exhibit an even stronger interaction with the $SiO_x$ substrate. We therefore assume that the substrate is covered with the polar middle blocks, resulting in a thin film structure that consists of a homogeneous B layer adsorbed at the substrate, covered with a laterally microphase-separated PS/PMMA surface layer. This notion is in agreement with the SFM results and follows the prediction based on SCF calculations of Pickett and Balazs[11] (see Scheme 4d). Given the rather short length of the middle blocks, however, we cannot exclude that part of the substrate is covered with PMMA as well. This would then lead to a compromise between the morphologies depicted in Scheme 4, parts b and d. In comparing experiment and theoretical prediction, one has to realize that the structures observed experimentally were formed during the dip-coating and subsequent drying process and did not change significantly on further annealing. It remains unclear though, whether they represent the thermodynamic equilibrium structure of the film. In contrast, the SCF calculations predict the equilibrium morphology based on the minimum of the free energy of the system.

**Ultrathin Films.** Ultrathin films were prepared by adsorption of the block copolymers from dilute (1 mg/mL) solutions in tetrahydrofuran (THF) onto polished silicon wafers. To ensure that only strongly physisorbed polymer molecules are present at the surface, the silicon wafer was rinsed thoroughly in pure THF after being removed from solution. Subsequently, the samples were dried at room temperature. THF was chosen because it dissolves the outer blocks of the different block copolymers well and therefore we do not expect micelle formation in solution. Detailed investigations on the solution properties are presently under way in order to illuminate the structure-forming process and will be described elsewhere. Thus, so far we can assume that the surface structures are formed by adsorption of individual block copolymer molecules. The dried films were investigated with SFM operated in tapping mode.

Figures 3 and 4 show a series of ultrathin block copolymer films from PS-*b*-PHEMA-*b*-PMMA and PS-*b*-P2VP-*b*-PMMA, respectively. All samples exhibit a striped surface morphology with characteristic values of half-width $R$, height $H$, and half-distance $D$ of the stripes. The molecular parameters as well as the $R$, $H$, and $D$ values are summarized in Table 3. The SFM phase images in Figure 3 demonstrate that at least two clearly distinguishable materials are found on the surface. The regions that appear brighter in the phase image correspond to materials which induce a higher phase shift ($\Delta\varphi$: 4−6°). As mentioned above, the larger phase shift is expected to occur on the harder material (PMMA). Height profiles over a surface area where the polymer has partially been removed by scratching with a needle confirm that the valleys are covered by an ultrathin polymer layer of thickness around 1−2 nm. Therefore, according to previous work on ultrathin films,[14,19,23] we assume a surface structure as depicted in Scheme 2 where the B and C blocks (PHEMA/P2VP-*b*-PMMA) are adsorbed to the polar substrate and PS protrusions form the characteristic stripes. Details of the morphology will be discussed later.

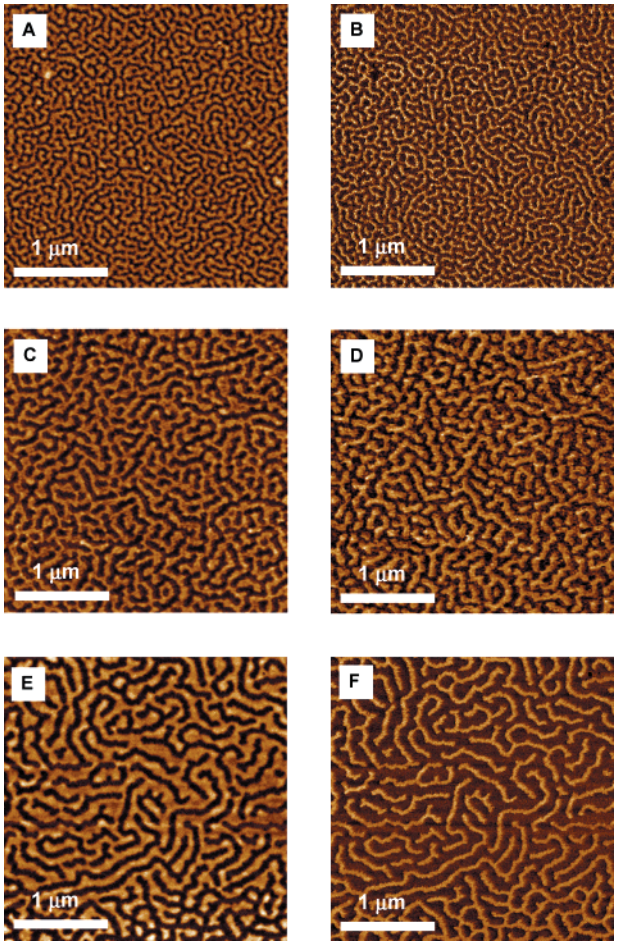


**Figure 3.** SFM micrographs and phase images of ultrathin films of PS-*b*-PHEMA-*b*-PMMA adsorbed from 1 mg/mL THF solutions onto a polished silicon wafer: (a, b) $S_{47}H_{10}M_{43}^{82}$; (c, d) $S_{46}H_4M_{50}^{134}$; (e, f) $S_{67}H_6M_{27}^{129}$. Topography: 8 nm, Phase: 15°.

Figure 3a shows an ultrathin film of $S_{47}H_{10}M_{43}^{82}$ (degrees of polymerization: 370/65/350). The sample exhibits a continuous stripelike surface pattern characterized by $H = 3.8 \pm 0.6$ nm, $D = 50 \pm 8$ nm, and $R = 29 \pm 5$ nm. The average half-width $R$ of a stripe has been estimated taking into account the convolution of the topographic profile with the curvature of the tip apex. If we picture the PS stripes as composed of many cylindrical caps of contact area $(2R)^2$ and height $H$ (Scheme 3) with a density $\rho = 1.1$ g/cm$^3$, the aggregation number $n_{PS}$ is estimated to be 140 ± 50. (The large uncertainty in $n_{PS}$ is caused by the difficulties involved in a precise determination of the stripe half-width $R$.)

The SFM topography image in Figure 3c shows an ultrathin film of $S_{46}H_4M_{50}^{134}$ (590/40/680). The sample exhibits the same typical characteristics as described

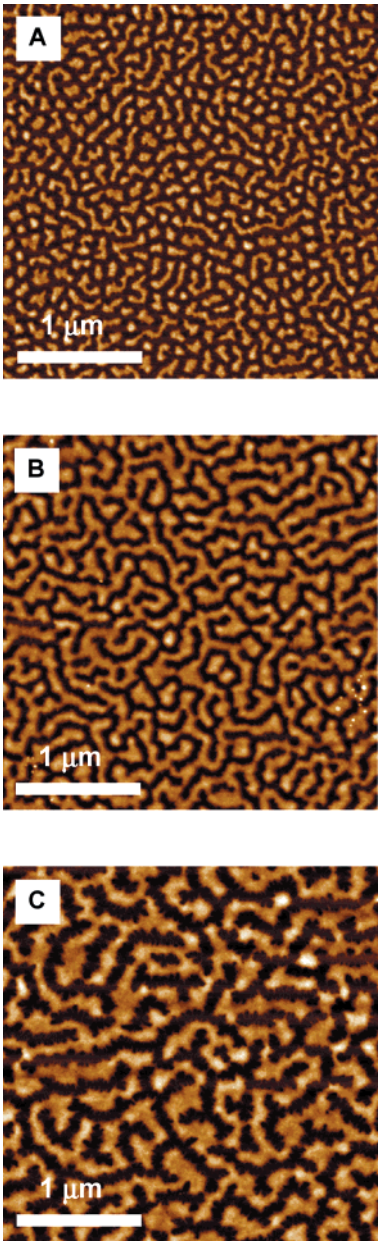


**Figure 4.** SFM micrographs of ultrathin films of PS-*b*-P2VP-*b*-PMMA adsorbed from 1 mg/mL THF solutions onto a polished silicon wafer: (a) $S_{51}2VP_5M_{44}^{110}$; (b) $S_{48}2VP_5M_{47}^{180}$; (c) $S_{56}2VP_6M_{38}^{299}$. *Z* range: 8 nm.

**Table 3. Characteristic Lateral Spacings of Phase-Separated Block Copolymers in Ultrathin Films Adsorbed from 1 mg/mL THF Solution Showing Stripe Morphology**[a]

| polymer | $N_S/N_{H/2VP}/N_M$ | *R* [nm] | *H* [nm] | *D* [nm] | $n_{PS}$ |
|---|---|---|---|---|---|
| $S_{47}H_{10}M_{43}^{82}$ | 370/65/350 | 29 ± 5 | 3.8 ± 0.6 | 50 ± 8 | 140 |
| $S_{46}H_4M_{50}^{134}$ | 590/40/680 | 44 ± 6 | 4.0 ± 0.8 | 73 ± 9 | 220 |
| $S_{67}H_6M_{27}^{129}$ | 830/60/340 | 53 ± 7 | 4.3 ± 0.8 | 90 ± 10 | 250 |
| $S_{51}2VP_5M_{44}^{110}$ | 540/55/480 | 38 ± 5 | 3.9 ± 0.8 | 64 ± 7 | 180 |
| $S_{48}2VP_5M_{47}^{180}$ | 825/80/855 | 50 ± 5 | 4.4 ± 0.6 | 80 ± 7 | 230 |
| $S_{56}2VP_6M_{38}^{299}$ | 1620/160/1140 | 73 ± 9 | 5.2 ± 1.2 | 125 ± 15 | 290 |

[a] $n_{PS}$ = average number of aggregated PS chains in a segment of a circle in cross-section with a basis of $2R \times 2R$ and a height *H* (error range ± 40%).

for $S_{47}H_{10}M_{43}^{82}$. The pattern is very regular in height, half-distance and half-width of the stripes which surround isolated valleys of PHEMA-*b*-PMMA. The respective values of *D*, *R*, *H*, and $n_{PS}$ are included in Table 3.

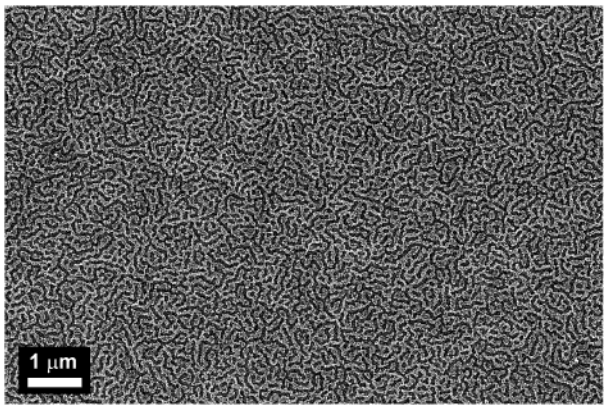


**Figure 5.** Large area SEM micrograph of an ultrathin film of $S_{48}2VP_5M_{47}^{180}$ adsorbed from 1 mg/mL THF solution onto a polished silicon wafer.

Figure 3e shows the topography image of $S_{67}H_6M_{27}^{129}$ (830/60/340) which again exhibits the regular and continuous stripe pattern. In addition, the film shows a tendency to breakup into an islandlike structure (lower right corner). We shall return to this issue below. Furthermore, a comparison with $S_{47}H_{10}M_{43}^{82}$ (Figure 3a) demonstrates the significant influence of the PS block on the half-distance *D* of the stripes.

Figure 4a shows an ultrathin film of $S_{51}2VP_5M_{44}^{110}$ (540/55/480). Compared to all other samples the stripes in this case are not continuous but broken up into long and short islands that still exhibit the characteristics of a stripe pattern. Half-width, half-distance and height are still uniform and correlate well with spacings found in the other samples as will be discussed further below. ($R = 38 \pm 5$ nm, $D = 64 \pm 7$ nm, and $H = 3.9 \pm 0.8$ nm.) The aggregation number $n_{PS}$ can be estimated to some 180 agglomerated PS chains.

The ultrathin film morphology of $S_{48}2VP_5M_{47}^{180}$ (825/80/855) is shown in Figure 4b. According to the expected behavior, the characteristic scales increase so that $R = 50 \pm 5$ nm and $D = 80 \pm 7$ nm. Besides the stripes some islandlike features are also detected that fit well to the overall scaling. The number of aggregated PS chains as defined above rises to $n_{PS} = 230$.

To show that the surface patterns indeed extend over large areas over the whole substrate, SEM pictures were taken. In Figure 5 an image of an ultrathin film of $S_{48}2VP_5M_{47}^{180}$ is shown. SEM has been chosen instead of a large area SFM image because high resolution images can be obtained easily capturing large areas. As the PS block has been stained with $RuO_4$ vapor prior to the measurement, the PS stripes appear brighter than the P2VP and PMMA sublayer. The haziness in the PS parts may be due to electron emission from the edges of the slightly rough PS stripes. The structure shown in Figure 5 demonstrates the large scale quality common to all surface structures reported on in this work.

The topographic SFM image of the polymer with the largest overall molecular weight $S_{56}2VP_6M_{38}^{299}$ (1620/160/1140) is shown in Figure 4c. As expected, the characteristic spacings are larger than in any other block copolymer investigated in this work. In addition, also the average aggregation number of a PS stripe increases considerably. The average *R*, *H*, *D*, and $n_{PS}$ values are given in Table 3. The SFM image shows that the half-width *R* of the PS stripes is not very uniform and the edges of the stripes appear to be rather rough. Another feature which appears more or less pronounced

in all ultrathin films is a partial undulation of the stripes. This undulation and the partial breakup of the stripes lead to the conclusion that the observed patterns may be metastable and may undergo a significant rearrangement under certain conditions (e.g., annealing or solvent vapor treatment).

As can be seen in Figures 3 and 4, the half-width $R$ of the PS stripes increases with increasing molecular weight of the PS block. The half-distance $D$, on the other hand, is controlled by the molecular weight of the PHEMA-*b*-PMMA and P2VP-*b*-PMMA blocks, respectively. Yet, at constant molecular weight of the PHEMA-*b*-PMMA blocks an increase of the degree of polymerization of the PS block also leads to a significantly larger value of $D$ (compare, e.g. $S_{47}H_{10}M_{43}^{82}$ (370/65/350), $D = 50 \pm 8$ nm, and $S_{67}H_6M_{27}^{129}$ (830/60/340), $D = 90 \pm 10$ nm). In addition, the aggregation number $n_{PS}$ nearly doubles from 140 to 250 agglomerated chains per stripe section.

Finally we note that the stripe to stripe distances (*2D*) in the ultrathin films are considerably larger than the respective bulk values. This widening of the structure indicates a significant stretching of the adsorbed blocks resulting in a quasi-2-dimensional surface layer, as will be discussed further below.

**Annealed Ultrathin Films.** As indicated by the undulations of the surface stripes found in the ultrathin film samples, the observed patterns may not represent the thermodynamically stable surface morphology. Consequently, the ultrathin films were annealed for 8 days at 170 °C in a vacuum oven. This temperature is 40−50 °C higher than the highest glass transition temperature ($T_g$) of the block copolymer components in the ultrathin films. The relatively high temperature was chosen with respect to the fact that the $T_g$'s in thin films can be significantly increased compared to the bulk values due to interactions between polar monomers and the substrate surface, whereas the reverse effect is expected for nonpolar monomers.[20−22]

In fact, on annealing we observe a clear transition from PS stripes to more or less round shaped PS islands as shown in Figure 6. The level of ordering is not very high, and additional annealing at the same temperature does not change the surface pattern any more. The characteristic spacings are listed in Table 4. The half-width $R$ of the round shaped PS aggregates was estimated assuming a circular basis with radius $R$. This estimate and the broad distribution of the size of the aggregates leads to the large error in $R$. Nevertheless, the SFM micrographs in Figure 6 exhibit a clear correlation of the radius $R$ and the height $H$ with the molecular weight of the PS block. Furthermore, it can be seen that the overall spacings between the agglomerates increase with increasing PHEMA/P2VP-*b*-PMMA block length. Compared to the surface patterns observed prior to annealing, the lateral spacing (i.e., the half-distance $D$) remains constant within the experimental error. Accordingly, the height values coincide with previous height data obtained from the stripe morphologies of the unannealed samples. In contrast, the average mean radii $R$ decreased significantly after annealing, especially for the formerly broad stripes. The overall impression is dominated by the observation that the radii of the clusters generated from stripes with large half-width are less uniform than for clusters resulting from smaller stripes (Figure 6, parts a and c).

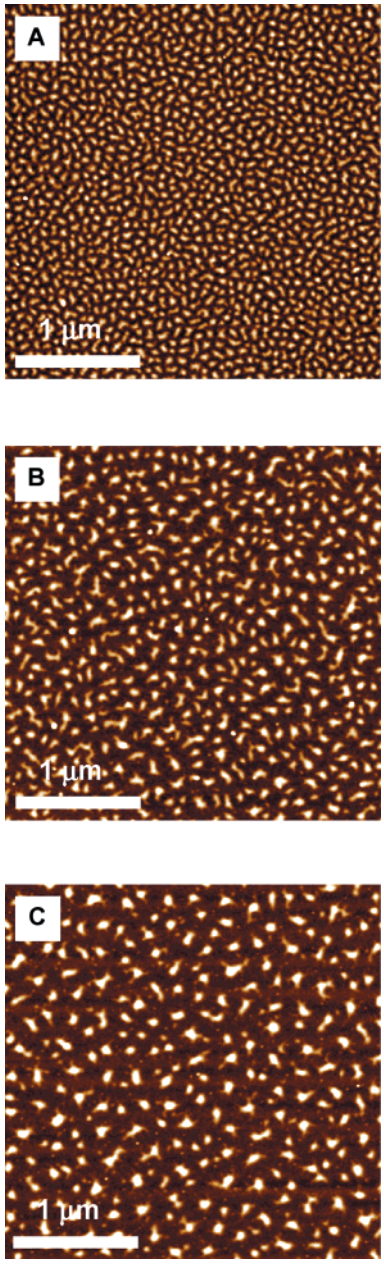


**Figure 6.** SFM micrographs of ultrathin films adsorbed from 1 mg/mL THF solutions onto a polished silicon wafer after annealing for 8 days at 170 °C in vacuum: (a) $S_{47}H_{10}M_{43}^{82}$ ($Z$ range: 6 nm); (b) $S_{67}H_6M_{27}^{129}$; (c) $S_{56}2VP_6M_{38}^{299}$. $Z$ range: 10 nm (b, c).

**Table 4. Characteristic Lateral Spacings of Phase-Separated Block Copolymers in Ultrathin Films Adsorbed from 1 mg/mL THF Solution, after Annealing at 170 °C for 8 days, Showing Island Morphology**

| polymer | $N_S/N_{H/2VP}/N_M$ | $R$ [nm][a] | $H$ [nm] | $D$ [nm] |
|---|---|---|---|---|
| $S_{47}H_{10}M_{43}^{82}$ | 370/65/350 | 23 ± 5 | 3.5 ± 0.5 | 42 ± 6 |
| $S_{46}H_4M_{50}^{134}$ | 590/40/680 | 32 ± 10 | 4.3 ± 0.8 | 63 ± 10 |
| $S_{67}H_6M_{27}^{129}$ | 830/60/340 | 34 ± 14 | 5.9 ± 1.1 | 81 ± 15 |
| $S_{51}2VP_5M_{44}^{110}$ | 540/55/480 | 27 ± 9 | 4.9 ± 1.0 | 55 ± 10 |
| $S_{48}2VP_5\ M_{47}^{180}$ | 825/80/855 | 30 ± 12 | 5.8 ± 1.0 | 78 ± 19 |
| $S_{56}2VP_6M_{38}^{299}$ | 1620/160/1140 | 36 ± 14 | 6.6 ± 1.0 | 104 ± 20 |

[a] Estimated from *nanoscope particle analysis* assuming a circular basis of the aggregates.

In addition, the average number of aggregated chains per cluster ranges between 50 and 90 with an estimated error of ±60%.

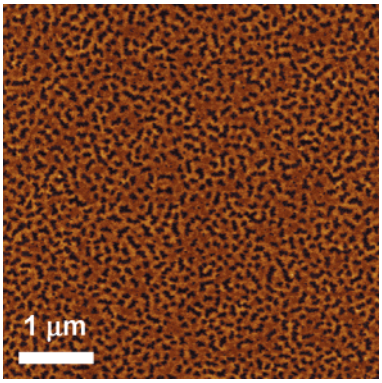


**Figure 7.** SFM micrograph of ultrathin film of $S_{48}2VP_5M_{47}^{180}$ dip-coated from a 0.1 mg/mL THF solution onto a polished silicon wafer. *Z* range: 8 nm.

We note in passing that a 7-day treatment in saturated THF vapor results in a morphological transition nearly identical to the one observed after annealing.

**Concentration Dependence of Pattern Formation.** When ultrathin films are prepared by dip-coating from 0.1 mg/mL solutions in THF onto polished silicon wafers, the surface patterns are very similar to the stripelike morphologies as prepared by adsorption from 1 mg/mL solutions in THF. In fact, the scaling of the lateral spacings is identical to the one found for the adsorbed films whereas the height values appear to be slightly larger. This may be due to a higher overall coverage. In addition, the as-prepared films exhibited a smooth and structureless surface. This finding may be attributed to a nearly complete PS coverage, which only partially dewetts the adsorbed sublayer. A few irregular holes are formed as shown in Figure 7. After exposue to saturated THF vapor for a few hours, the PS surface layer completely brakes up to form the well-known stripelike patterns. Similarly, annealing also leads to a morphological transition resulting in an islandlike morphology.

When samples were prepared by dip-coating from 0.01 mg/mL solutions in THF onto polished silicon wafers, an irregular pattern of small elongated or oval islands was observed. Two samples ($S_{46}H_4M_{50}^{134}$ (590/40/680) and $S_{48}2VP_5M_{47}^{180}$ (825/80/855)) were used for these studies. The islands had a diffuse shape at their base, which may be attributed to bundles of polymer chains (Figure 8a/b). Apparently, the substrate is not covered completely by the polymer but very small aggregates of polymer chains are spread all over the wafer. The mean height of the main clusters for $S_{46}H_4M_{50}^{134}$ was determined to be $2 \pm 1$ nm, excluding all objects with $H < 0.5$ nm. A similar result was obtained for the as-prepared adsorbates of $S_{48}2VP_5M_{47}^{180}$ (see Table 5).

After annealing for 5 days at 190 °C, an array of more regularly round shaped polymer clusters is formed (Figure 8, parts c and d). The mean radii *R* were determined to be $20 \pm 6$ nm and $25 \pm 8$ nm for $S_{46}H_4M_{50}^{134}$ and $S_{48}2VP_5M_{47}^{180}$, respectively. No significant change in the lateral spacing was found on further annealing. However, the height of the clusters changed significantly which may be attributed to an incorporation of the small molecule bundles spread on the surface, thus increasing the cluster height and volume. This is also supported by the small decrease in the overall number of clusters higher than 0.5 nm which changes from ~1200 to ~1100 and from ~850 to ~700 for $S_{46}H_4M_{50}^{134}$ and $S_{48}2VP_5M_{47}^{180}$, respectively (Table 5). The calculation of the aggregation number $n_{PS}$ gives a value of 25 and 40 chains per cluster with an error range of ±65%.

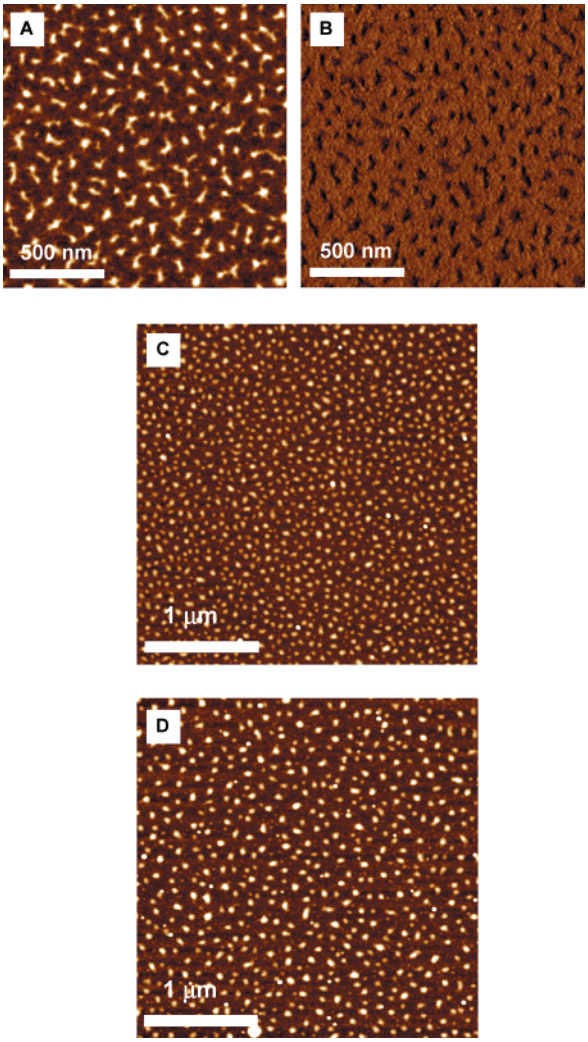


**Figure 8.** SFM micrographs of ultrathin films dip-coated from 0.01 mg/mL THF solutions onto a polished silicon wafer: $S_{46}H_4M_{50}^{134}$ (a) topography (5 nm) and (b) phase (15°) as-prepared and (c) after annealing for 5 days at 190 °C; (d) $S_{48}2VP_5M_{47}^{180}$ after annealing for 5 days at 190 °C. *Z* range: 10 nm (c, d).

**Table 5. Characteristic Lateral Spacings of Phase-Separated Block Copolymers in Ultrathin Films Adsorbed from 0.01 mg/mL THF Solution Showing Island Morphology before and after Annealing at 190 °C for 5 days**

| polymer | $N_S/N_{H/2VP}/N_M$ | *R* [nm] | *H* [nm] | *D* [nm] | no. of clusters [3 × 3 μm²] |
|---|---|---|---|---|---|
| $S_{46}H_4M_{50}^{134}$ | 590/40/680 | 19 ± 14 | 2 ± 1 | 56 ± 14 | ≈1200 |
| after annealing | | 20 ± 6 | 4 ± 1 | 50 ± 12 | ≈1100 |
| $S_{48}2VP_5M_{47}^{180}$ | 825/80/855 | 20 ± 12 | 2 ± 1 | 74 ± 15 | ≈850 |
| after annealing | | 25 ± 8 | 5 ± 2 | 75 ± 18 | ≈700 |

These findings underline the fact that the amount of polymer deposited during dip-coating is not sufficient to cover the surface completely. Because of the lack of polymeric material, the most favorable form for the aggregates on the surface is given by a drop- or islandlike agglomeration.

**Scaling Analysis.** Recently, Potemkin et al. developed a theory predicting the scaling parameters of surface patterns observed in ultrathin films of PS-*b*-

P2VP and PS-*b*-P4VP diblock copolymers.[13,14] In this system the PVP blocks adsorb to the substrate and the PS blocks dewet from the PVP sublayer. The degree of polymerization and the surface energies (with $\gamma_{PVP} > \gamma_{PS}$) of both blocks were found to affect the size and shape of the observed structures, i.e., island or stripe morphologies of different spacings. Their calculations resulted in the following dependences:

$$R,H \propto (N_A{}^{d-3} N_B{}^{d+1})^{1/(3d-1)} \quad (3a)$$

$$D \propto (N_A{}^{d+1} N_B{}^{d-1})^{1/(3d-1)} \quad (3b)$$

with $d = 3$ for island and $d = 2$ for stripe morphologies, where $N_A$ is the degree of polymerization (DP) of the adsorbing block (in their case PVP) and $N_B$ the DP of the protruding block (PS), which leads to

$$R,H \propto N_A{}^{-0.2} N_B{}^{0.6} \quad (4a)$$

$$D \propto N_A{}^{0.6} N_B{}^{0.2} \quad (4b)$$

for a stripe morphology and

$$R,H \propto N_B{}^{0.5} \quad (5a)$$

$$D \propto N_A{}^{0.5} N_B{}^{0.25} \quad (5b)$$

for an island morphology.

Given the rather short length of the middle blocks in our study and the fact that the PMMA end blocks are expected to adsorb onto a polar substrate as well, we shall try to model our system by treating blocks B and C as a single adsorbing unit and use the above theoretical approach. This choice is further corroborated by the surface energy differences between the blocks, which fulfill the assumption of the above model, i.e., $\gamma_{PHEMA,PMMA} > \gamma_{PS}$ and $\gamma_{P2VP,PMMA} > \gamma_{PS}$.

**Striped Patterns.** In Figure 9 the scaling behavior of half-width *R*, half-distance *D*, and height *H* are compared to the above theory. The axes of the graphs are scaled in a way that the experimental points should fall onto straight lines. As can be seen in Figure 9a the scaling of the half-width *R* of the stripes is well described by the theory. The line drawn in the plot is calculated by linear regression. Stripe heights *H* (Figure 9c), which are expected to scale identically to the half-width *R*, also agree quite well with theory even though the accuracy is not as good as for the *R* values or the half-distance *D*. Obviously, the nature of the middle block B (PHEMA or P2VP) does not seem to have a strong influence on the scaling behavior of *R* and *H* as especially $S_{46}H_4M_{50}{}^{134}$ (590/40/680) and $S_{51}2VP_5M_{44}{}^{110}$ (540/55/480) as well as $S_{67}H_6M_{27}{}^{129}$ (830/60/340) and $S_{48}2VP_5M_{47}{}^{180}$ (825/80/855) exhibit an interesting similarity in half-width and height. They only differ significantly in the length of the PMMA block which contributes to a different scaling behavior with regard to *D*. In Figure 9b the strong influence of the PS molecular weight on the stripe to stripe distance *D* can be seen. The asymmetrical polymer $S_{67}H_6M_{27}{}^{129}$ (830/60/340) shows a very large stripe-to-stripe half-distance *D* which is about 1.6 times larger than expected according to the line calculated using linear regression disregarding $S_{67}H_6M_{27}{}^{129}$ (hollow square). Compared to the sample $S_{47}H_{10}M_{43}{}^{82}$ (370/65/350), the molecular weight of the adsorbing blocks B/C is nearly constant so that the only difference is given by the PS block which is 2.25 times larger. This phenomenon has been observed earlier in the case of asymmetric PS-*b*-P2VP diblock copolymers with a ratio N(PS):N(P2VP) of approximately 3:1 which is similar to the ratio N(PS):N(PHEMA/PMMA) in $S_{67}H_6M_{27}{}^{129}$ (830/60/340).[14] A possible explanation for the above observation could be that in this case, there is not a homogeneous PHEMA-*b*-PMMA sublayer below the PS stripes but a certain area where PS is in direct contact with the silicon substrate.[14] If the linear regression is carried out without the *D* value of polymer $S_{67}H_6M_{27}{}^{129}$, one finds very good qualitative agreement with the scaling prediction.

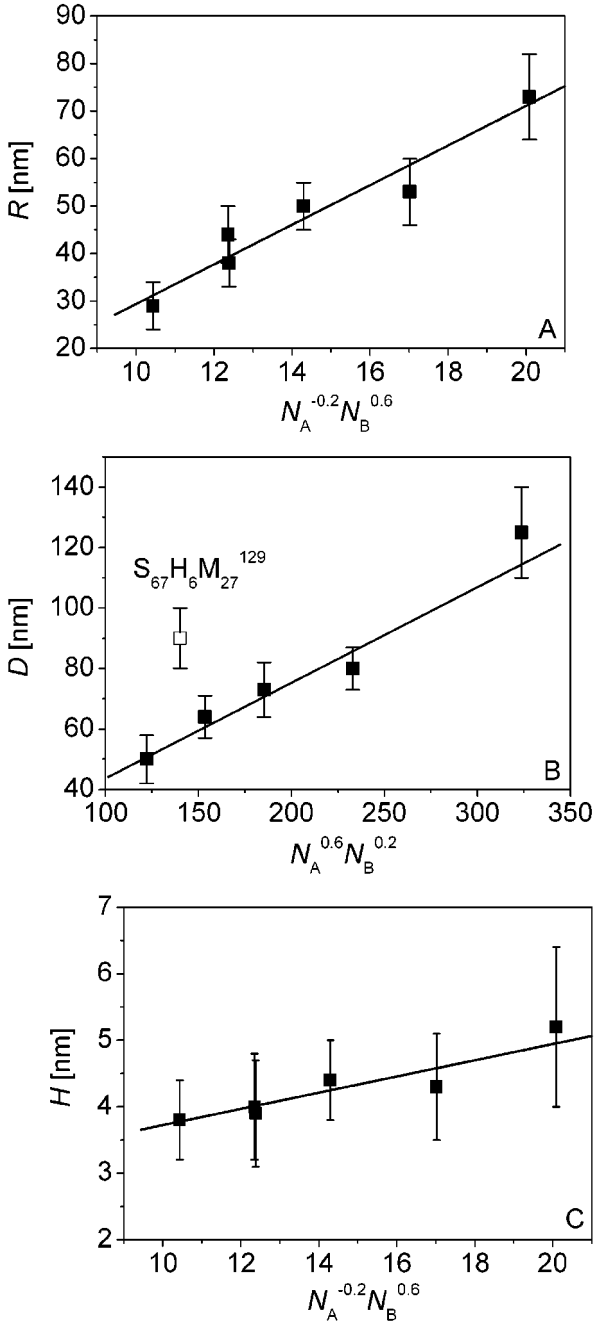


**Figure 9.** Scaling of PS-*b*-PHEMA-*b*-PMMA and PS-*b*-P2VP-*b*-PMMA stripe morphology: (a) half-width *R*; (b) half-distance *D*; (c) height *H* of PS stripes.

**Islandlike Patterns.** In the following, we compare the measured *R*, *H*, and *D* values of the islandlike

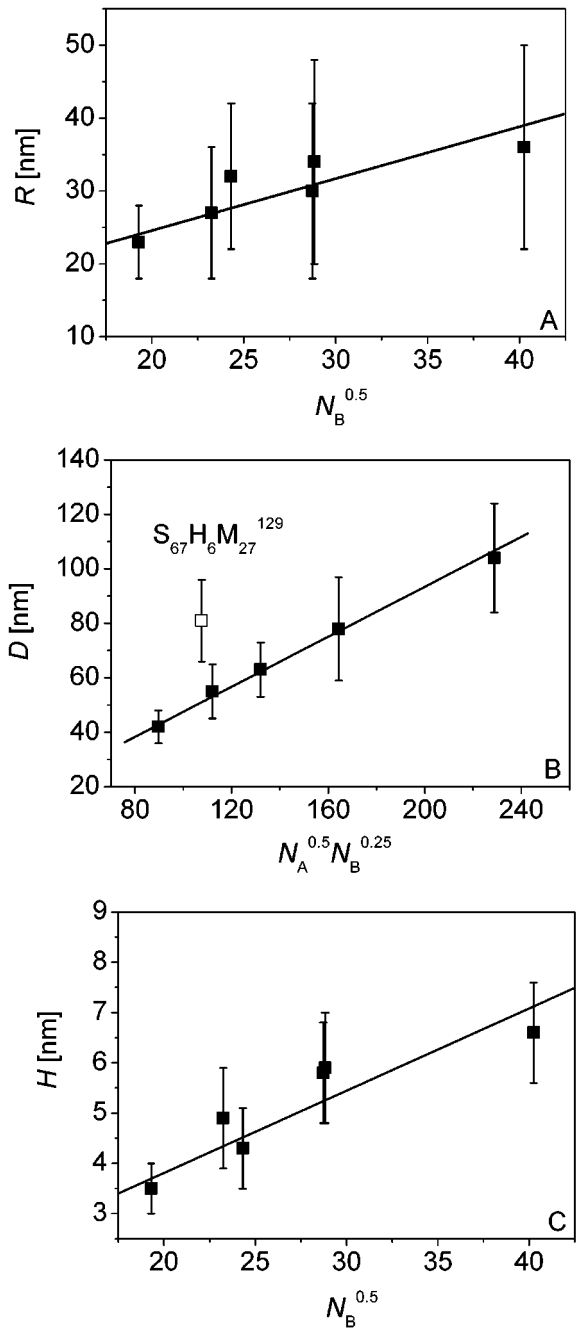


**Figure 10.** Scaling of PS-*b*-PHEMA-*b*-PMMA and PS-*b*-P2VP-*b*-PMMA island morphology: (a) half-width *R*; (b) half-distance *D*; (c) height *H* of PS islands.

surface patterns with the theory by Potemkin et al.[13] using eq 5, parts a and b. Figure 10 shows a series of graphs where the radii *R*, half-distances *D*, and heights *H* are plotted such that the data points should fall onto straight lines. The black line drawn in the plots is calculated according to linear regression. Both the radius *R* and the height *H* (Figure 10, parts a and c) are expected to depend on the PS molecular weight only and should scale as $N_{PS}^{0.5}$. This is indeed observed. The large error bars reflect the broad distribution of the cluster radii and the difficulties in the correct determination of *R* as described earlier. The height values are more reliable and have a much smaller error range. Besides, like in the case of the stripe morphology, we find similarities in the characteristic spacings especially for $S_{46}H_4M_{50}^{134}$ (590/40/680) and $S_{51}2VP_5M_{44}^{110}$ (540/55/480) as well as for $S_{67}H_6M_{27}^{129}$ (830/60/340) and $S_{48}2VP_5M_{47}^{180}$ (825/80/855) which both have PS blocks of similar length. As expected, the radius *R* and the height *H* are nearly identical without any influence induced by the different B/C block composition. As our results show a qualitatively good agreement between the scaling predictions for the observed structures ($R,H \propto N_{PS}^{0.5}$) and the actual radius and height of the clusters, we may conclude that the conformation of the PS chains in an aggregate is nearly Gaussian.

The half-distance *D* of the PS aggregates scales nearly perfectly according to the theoretical predictions (Figure 10b). If one compares the ultrathin annealed film of $S_{47}H_{10}M_{43}^{82}$ (370/65/350) to $S_{67}H_6M_{27}^{129}$ (830/60/340) as shown in Figure 6, parts a and b, it turns out that an increase of the degree of polymerization of the PS block at a constant molecular weight of the PHEMA-*b*-PMMA blocks leads to a significantly larger value of *D* which increases from $D = 42 \pm 6$ to $81 \pm 15$ nm. The lateral spacing in the latter case is 1.6 times larger than expected according to the black line given by the linear fit. This is a very similar deviation as measured for the stripelike morphology. A possible explanation for this phenomenon has already been given for the same observation made in films with stripe morphology and therefore will not be discussed further.

In the following, we shall discuss the scaling behavior of the above-described ultrathin film morphologies. On the basis of previous investigations on ultrathin films of PS-*b*-P2VP and PS-*b*-P4VP[14,19,23] we expect the observed structures to consist of PS stripes with a mixed sublayer of PMMA and PHEMA or P2VP, respectively. The good agreement of our results to the scaling analysis developed for diblock copolymers corroborates this notion. Obviously, once in contact with the silicon wafer, the polarity of both the middle blocks and the PMMA end block leads to coadsorption to the substrate surface, resulting in a quasi-2-dimensional layer of the PHEMA-*b*-PMMA and P2VP-*b*-PMMA portion of the block copolymers. Because of the unfavorable interaction and elastic contributions to the free energy (see below), the PS blocks do not cover this layer completely but rather dewet the sublayer. During this process, the PS chains form aggregates of different size and spacing resulting in the three-dimensional structures observed in the SFM images. The size, height, and half-distance of the resulting structures clearly depend on the PS/PMMA block length as shown in Table 3. The definition of the parameters used for scaling analysis and a cross section of the morphology are depicted in Scheme 2 which summarizes schematically the above descriptions.

So far only the dimensions associated with the PS stripes were considered. One can easily calculate the half-width of the valleys between adjacent stripes, which should consist mainly of PMMA, from the difference of the *D* and *R* values summarized in Table 3. It is interesting to compare these values to the radii of gyration of the PMMA block. As an example, for $S_{48}2VP_5M_{47}^{180}$ (825/80/855) the radius of gyration of the PMMA block is about 8 nm, whereas the half-width of the valleys found in the corresponding ultrathin film amounts to some 30 nm. This result indicates significant streching of the PMMA chains in the adsorbed layer. The free energy cost due to stretching must therefore be balanced by maximizing the number of contacts to the substrate and the corresponding adhesion energy. To cover the PMMA layer in the valleys completely, the

PS chains ($R_g \sim 8$ nm) would have to stretch approximately 4 times as well. Since no enthalpic gain of comparable magnitude is expected at the PS/PMMA interface, complete coverage of PMMA by PS is not observed. From the *D* and *R* data for the other block copolymers we consistently find a streching of the adsorbing blocks by about 4−5 times compared to an unperturbed Gaussian chain. The half-width of the observed valleys is 6 times smaller compared to the respective PMMA contour length. Together with the average thickness of the adsorbed polymer layer of approximately 1−2 nm, we may conclude that the adsorbed coils form trains and loops on the substrate surface as shown in Scheme 2.

In the case of $S_{67}H_6M_{27}^{129}$ (830/60/340) the picture is quite different. As indicated earlier the unusually large spacing of the PS stripes could be due to an incomplete coverage of the substrate by a PHEMA-*b*-PMMA sublayer. This assumption is further supported by the fact that the adsorbed blocks would have to be stretched more than 8 times (which is half the contour length) in order to form a complete sublayer. It is questionable whether the corresponding entropic energy cost can be compensated for by the adhesion energy. Therefore, partial coverage of the substrate by the PS chains and a reduced stretching of the PMMA coils seems to be a more favorable condition.

After annealing, the ultrathin films show significant morphological changes with the striped surface pattern turning into an islandlike surface structure. This behavior indicates that the striped patterns do not correspond to the thermodynamically stable morphology. In contrast to other investigations on ultrathin block copolymer films,[24] the size of the clusters is not very uniform and only a poor long range order develops. We may assume that this observation is related to the properties of the substrate, following the results of Spatz et al., who found a pronounced influence of the substrate on the size and uniformity of PS-*b*-P2VP clusters on mica and GaAs surfaces, respectively.

Furthermore, according to recent calculations by Potemkin et al.[13] on the stability of islands and stripes and the transition between both phases, we expect that our system is located close to the phase transition between stripes and islands. One important factor that accounts for the stability of one phase is given by the difference in surface tension of the dominant blocks. Compared to the system PS-*b*-P2VP ($\Delta\gamma \approx 50$ mN/m[25]) the difference in surface tension between PS and PMMA only amounts to $\Delta\gamma \approx 0.4-20.2$ mN/m depending on the amount of moisture absorbed by PMMA (0−3%).[25] According to the predictions of Potemkin et al.,[13] stripes are more stable for $\gamma$(adsorbing block/air) > $\gamma$(dewetting block/air), which would result in a smaller surface area to be covered by the adsorbing block. The larger the difference in surface tension, the more energetically favorable is the striped structure. On the other hand, the islandlike pattern would be more stable if the surface tension ratio was reverse. A difference in surface tension as small as described above does not provide a thermodynamic argument to decide in favor of one or the other morphology.

Another hint pointing toward an instability of the observed stripe morphology is given by the scaling behavior of the stripe dimensions *H* and *R*, respectively. For a state close to the transition regime a Gaussian behavior of *H* and *R* is expected ($R,H \propto N_{PS}^{0.5}$).[13] As shown in Figure 11, this is indeed observed. The fit for the islandlike morphology obtained after annealing the striped samples (Figure 10) does not show such a good agreement with theory, which can be explained by the large errors due to the nonuniformity of the clusters.

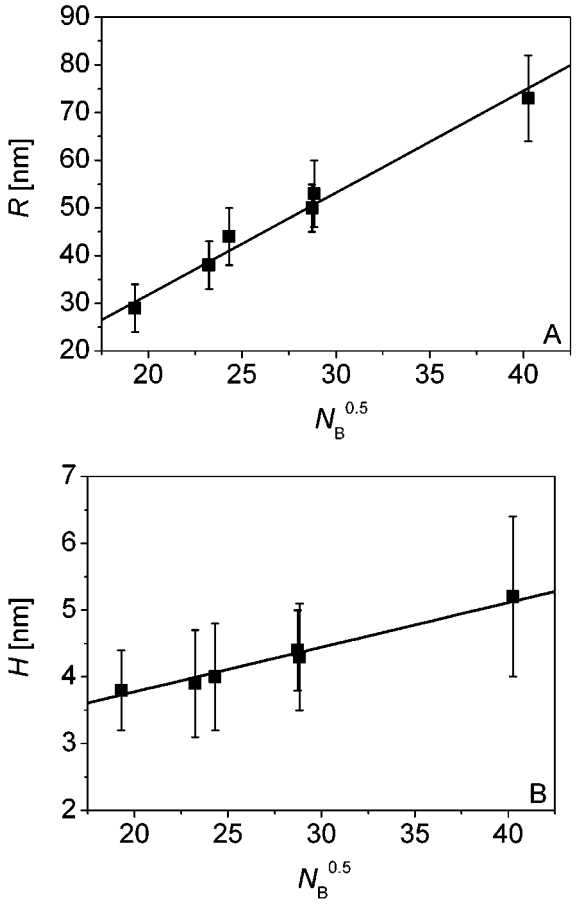


**Figure 11.** Scaling of PS-*b*-PHEMA-*b*-PMMA and PS-*b*-P2VP-*b*-PMMA stripe morphology according to Gaussian behavior: (a) half-width *R*; (b) height *H* of PS stripes.

A transition from stripes to islands has already been observed earlier by changing the overall molecular weight ratios,[13] but in the present study the transition is induced by instabilities resulting from the fact that the corresponding block copolymers are located in a region near the phase boundary between the two phases.

## Conclusions

We have shown that thin and ultrathin films of polystyrene-*b*-poly(2-vinylpyridine)-*b*-poly(methyl methacrylate) and polystyrene-*b*-poly(2-hydroxyethyl methacrylate)-*b*-poly(methyl methacrylate) block copolymers reveal regular surface patterns with worm-, stripe-, and islandlike morphologies. The characteristic spacings can be controlled via the molecular weight of the different blocks of the respective copolymers.

*Thin films* prepared by dip-coating from a polymer solution were found to exhibit a phase-separated wormlike surface morphology that presumably only consists of PS and PMMA microdomains with a characteristic lateral length scale similar to the bulk period $L_0$. We assume that the generation of such a striped surface pattern can be explained by complete coverage of the silicon oxide surface by PHEMA or P2VP, resulting in a thin film structure that consists of a homogeneous

layer of the middle block adsorbed at the substrate covered with a laterally microphase-separated surface layer of PS and PMMA microcomains. The proposed model for this morphology is in agreement with previous SCF calculations by Pickett and Balazs.[11]

In the case of the *ultrathin films*, our results demonstrate that adsorption of a block copolymer as an ultrathin film leads to a periodic surface domain structure (stripes), where both polar blocks (B and C) adsorb to the surface. Because of significant stretching of the adsorbed blocks the spacings between the domains are large for the rather low molecular weight block copolymers. The lateral dimensions correlate well with the molecular dimensions of the A and B/C blocks according to previously derived scaling laws.[13]

It could be shown that the striped structure observed in the as-prepared samples exhibits the tendency to rearrange into a thermodynamically more stable island-like structure on annealing. These patterns show a lower uniformity in size and long-range order, presumably due to the influence of the silicon substrate.

In particular, for ultrathin films, our results show that the size of the PS domains is dominated by the molecular weight of PS whereas the spacing of the PS stripes or clusters can be controlled by the length of the PHEMA-*b*-PMMA and P2VP-*b*-PMMA blocks. The understanding of domain formation by self-assembly of block copolymers into certain surface morphologies by tailoring the polymer architecture is an important aspect for future investigations on generation of polymeric templates for a large variety of applications.

**Acknowledgment.** The authors thank C. Drummer (BIMF) and A. Göpfert for their skillful help with SEM and TEM measurements, respectively. This work was financially supported by the Deutsche Forschungsgemeinschaft within the Schwerpunktsprogramm "Benetzung und Strukturbildung an Grenzflächen" (KR 1369/9). A.B. acknowledges a Kekulé fellowship by the Stiftung Stipendien-Fonds des Verbandes der Chemischen Industrie and the German Bundesministerium für Bildung und Forschung (BMBF).

## References and Notes

(1) Kellogg, G. J.; Walton, D. G.; Mayes, A. M.; Lambooy, P.; Russel, T. P.; Gallagher, P. D.; Satija, S. K. *Phys. Rev. Lett.* **1996**, *76*, 2503.

(2) Morkved, T. L.; Lu, M.; Urbas, A. M.; Ehrichs, E. E.; Jaeger, H. M.; Mansky, P.; Russell, T. P. *Science* **1996**, *273*, 931.

(3) Walton, D. G.; Kellogg, G. J.; Mayes, A. M.; Lambooy, P.; Russell, T. P. *Macromolecules* **1994**, *27*, 6225.

(4) Henkee, C. S.; Thomas, E. L.; Fetters, L. J. *J. Mater. Sci.* **1988**, *23*, 1685.

(5) Morkved, T. L.; Jaeger, H. M. *Europhys. Lett.* **1997**, *40*, 643.

(6) Singhvi, R.; Kumar, A.; Lopez, G. P.; Stephanopoulos, G. N.; Wang, D. I. C.; Whitesides, G. M.; Ingber, D. E. *Science* **1994**, *264*, 696.

(7) Morkved, T. L.; Wiltzius, P.; Jaeger, H. M.; Grier, D.; Witten, T. *Appl. Phys. Lett.* **1994**, *64*, 422.

(8) Spatz, J. P.; Roescher, A.; Möller, M. *Adv. Mater.* **1996**, *8*, 337.

(9) Spatz, J. P.; Eibeck, P.; Mössmer, S.; Möller, M.; Herzog, T.; Ziemann, P. *Adv. Mater.* **1998**, *10*, 849.

(10) Fukunaga, K.; Elbs, H.; Krausch, G. *Langmuir* **2000**, *16*, 3774.

(11) Pickett, G. T.; Balazs, A. C. *Macromol. Theory Simul.* **1998**, *7*, 249.

(12) Elbs, H.; Fukunaga, K.; Stadler, R.; Sauer, G.; Magerle, R.; Krausch, G. *Macromolecules* **1999**, *32*, 1204.

(13) Potemkin, I. I.; Kramarenko, E. Y.; Khokhlov, A. R.; Winkler, R. G.; Reineker, P.; Eibeck, P.; Spatz, J. P.; Möller, M. *Langmuir* **1999**, *15*, 7290.

(14) Eibeck, P.; Spatz, J. P.; Potemkin, I. I.; Kramarenko, E. Y.; Khokhlov, A. R.; Möller, M. *Polym. Prepr.* **1999**, *40*, 990.

(15) Hirao, A.; Kato, H.; Yamaguchi, K.; Nakahama, S. *Macromolecules* **1986**, *19*, 1294.

(16) Walheim, S.; Böltau, M.; Mlynek, J.; Krausch, G.; Steiner, U. *Macromolecules* **1997**, *30*, 4995.

(17) Morkved, T. L.; Lopes, W. A.; Hahm, J.; Sibener, S. J.; Jaeger, H. M. *Polymer* **1998**, *39*, 3871.

(18) Fasolka, M. J.; Banerjee, P.; Mayes, A. C.; Pickett, G.; Balazs, A. C. *Macromolecules* **2000**, *33*, 5702.

(19) Spatz, J. P.; Möller, M.; Noeske, M.; Behm, R. J.; Pietralla, M. *Macromolecules* **1997**, *30*, 3874.

(20) Keddie, J. L.; Jones, R. A. L. *Isr. J. Chem.* **1995**, *35*, 21.

(21) Keddie, J. L.; Jones, R. A. L.; Cory, R. A. *Faraday Discuss., Chem. Soc.* **1994**, *98*, 219.

(22) Fryer, D. S.; Nealey, P. F.; de Pablo, J. J. *Macromolecules* **2000**, *33*, 6439.

(23) Spatz, J. P.; Sheiko, S.; Möller, M. *Adv. Mater.* **1996**, *8*, 513.

(24) Spatz, J. P.; Eibeck, P.; Mössmer, S.; Möller, M.; Kramarenko, E. Y.; Khalatur, P. G.; Potemkin, I. I.; Winkler, R. G.; Reineker, P. *Macromolecules* **2000**, *33*, 150.

(25) Brandrup, J.; Immergut, E. H. *Polymer Handbook*, 3rd ed.; Wiley: New York, 1991.

MA002198D